frontiers | Frontiers in Plant Science

TYPE Original Research
PUBLISHED 28 July 2023
DOI 10.3389/fpls.2023.1170448

Check for updates

OPEN ACCESS

EDITED BY
Aliki Xanthopoulou,
Hellenic Agricultural Organisation (HAO), Greece

REVIEWED BY
Prabhakaran Soundararajan,
National Institute of Plant Genome Research (NIPGR), India
Victor Manuel Rodriguez,
Spanish National Research Council (CSIC), Spain
Wagner L. Araújo,
Universidade Federal De Viçosa, Brazil

*CORRESPONDENCE
R. Glen Uhrig
ruhrig@ualberta.ca

RECEIVED 23 February 2023
ACCEPTED 26 June 2023
PUBLISHED 28 July 2023

CITATION
Scandola S, Mehta D, Castillo B, Boyce N and Uhrig RG (2023) Systems-level proteomics and metabolomics reveals the diel molecular landscape of diverse kale cultivars. *Front. Plant Sci.* 14:1170448. doi: 10.3389/fpls.2023.1170448

COPYRIGHT
© 2023 Scandola, Mehta, Castillo, Boyce and Uhrig. This is an open-access article distributed under the terms of the Creative Commons Attribution License (CC BY). The use, distribution or reproduction in other forums is permitted, provided the original author(s) and the copyright owner(s) are credited and that the original publication in this journal is cited, in accordance with accepted academic practice. No use, distribution or reproduction is permitted which does not comply with these terms.

Systems-level proteomics and metabolomics reveals the diel molecular landscape of diverse kale cultivars

Sabine Scandola, Devang Mehta, Brigo Castillo, Nicholas Boyce and R. Glen Uhrig*

Department of Biological Sciences, University of Alberta, Edmonton, AB, Canada

Kale is a group of diverse *Brassicaceae* species that are nutritious leafy greens consumed for their abundance of vitamins and micronutrients. Typified by their curly, serrated and/or wavy leaves, kale varieties have been primarily defined based on their leaf morphology and geographic origin, despite having complex genetic backgrounds. Kale is a very promising crop for vertical farming due to its high nutritional content; however, being a non-model organism, foundational, systems-level analyses of kale are lacking. Previous studies in kale have shown that time-of-day harvesting can affect its nutritional composition. Therefore, to gain a systems-level diel understanding of kale across its wide-ranging and diverse genetic landscape, we selected nine publicly available and commercially grown kale cultivars for growth under near-sunlight LED light conditions ideal for vertical farming. We then analyzed changes in morphology, growth and nutrition using a combination of plant phenotyping, proteomics and metabolomics. As the diel molecular activities of plants drive their daily growth and development, ultimately determining their productivity as a crop, we harvested kale leaf tissue at both end-of-day (ED) and end-of-night (EN) time-points for all molecular analyses. Our results reveal that diel proteome and metabolome signatures divide the selected kale cultivars into two groups defined by their amino acid and sugar content, along with significant proteome differences involving carbon and nitrogen metabolism, mRNA splicing, protein translation and light harvesting. Together, our multi-cultivar, multi-omic analysis provides new insights into the molecular underpinnings of the diel growth and development landscape of kale, advancing our fundamental understanding of this nutritious leafy green super-food for horticulture/vertical farming applications.

KEYWORDS

kale, BoxCar DIA proteomics, GC-MS metabolomics, *Brassica oleracea*, diel plant biology

Introduction

Brassica oleracea and its diverse cultivar groups represent an important food crop for multiple populations across the globe. These include seven major cultivar groups: cauliflower, collard greens, broccoli, kohlrabi, cabbage, brussels sprouts and kale. Together, these crops represented 70.1 million metric tonnes of production in 2019 (https://www.fao.org/faostat/en/#data/QCL). Kale, which encompass several leafy *Brassicaceae* species (*B. oleracea* and *B. napus*) (Reda et al., 2021), is often referred to as a 'super-food' (Samec et al., 2019) as it is rich in numerous antioxidants (carotenoids, flavonoids, glucosinolates) and essentials vitamins (A, K and C), minerals (calcium and iron), dietary fibers (Becerra-Moreno et al., 2014) and low molecular weight carbohydrates (Megias-Perez et al., 2020). Additionally, kale has notable cultivation advantages, including a wide-ranging temperature tolerance that guarantees year-round availability in most climates (Samec et al., 2019). Given these characteristics, kale represents a horticultural crop with the potential to be a source of essential nutrients for multiple global populations (Migliozzi et al., 2015).

To maximize growth and to execute developmental programs, plants require the precise timing of diel (daily) events. Correspondingly, diel events are coordinated by a combination of circadian and light responsive mechanisms, which play a major role in modulating the plant cell environment at all molecular levels (Mehta et al., 2021). For example, in the model plant and related *Brassicaceae*, *Arabidopsis thaliana* (Arabidopsis), it is estimated that the circadian clock controls the diel expression of 1/3 of all genes (Covington et al., 2008). Further, the importance of the circadian clock and diel biology in plants is emphasized by its central role in governing critical agronomic traits such as biomass, flowering time and disease resistance (Creux and Harmer, 2019), suggesting diel biology should be a central facet of next-generation cropping systems (Hotta, 2021; Steed et al., 2021). This is particularly key for kale, which has shown that time-of-day harvesting can affect its nutritional composition (Casajus et al., 2021; Francisco and Rodriguez, 2021), indicating that time-of-day harvesting and postharvest storage is central to enhanced kale nutrition and shelf life when going to market (Reda et al., 2021). Currently, our understanding of kale rests at the production-level, with the diel molecular mechanisms underpinning unique and beneficial morphological and nutritional differences between kale cultivars remaining largely unknown (Megias-Perez et al., 2020).

To date, systemic molecular analyses of kale cultivars *convar. acephala* (Jin et al., 2018; Liu et al., 2020; Liu et al., 2021) var. *sabellica* (Pongrac et al., 2019) and *B. napus* var. *pabularia* (Chiu et al., 2018) have been limited, with no studies examining multiple cultivars or quantifying diel molecular changes. In one transcriptomic study of *B. oleracea convar. acephala* cultivars, glucosinolate, carotenoid and phenylpropanoid biosynthetic pathways were highlighted as critical in defining the differences between green 'manchoo collar' and red 'jeok seol' cultivars (Jeon et al., 2018). To date however, no investigations of *B. oleracea* var. *palmifolia* have been performed, limiting our molecular knowledge of these widely produced and consumed kale cultivars. This set of molecular studies has however demonstrated that kale is a highly dynamic and diverse set of species that requires a systemic, multi-omics investigation of multiple kale cultivars in order to elucidate diel molecular landscape features that can be harnessed for increased production and nutrition.

Light spectra, intensity and photoperiod have each been shown to be important in kale cultivation as modulators of the kale metabolome (Carvalho and Folta, 2014). Light is also essential for plant growth and development as it is a primary entrainment mechanism of the circadian rhythm of plants (Xu et al., 2022). With the circadian clock and diel plant cell regulation governing numerous agronomic traits of interest, including: flowering time, growth and plant defense (Steed et al., 2021), elucidating where changes in the molecular landscape of diverse kale genetics manifests through a diel/circadian lens using quantitative, systems-level omics technologies, represents a critical endeavour for optimizing the growth and nutrient content of kale grown in controlled growth environments.

Therefore, using a combination of gas-chromatography mass spectrometry (GC-MS) and the latest data independent acquisition (DIA) quantitative proteomics workflow called BoxCarDIA (Mehta et al., 2022), we establish the diel metabolome and proteome landscapes of nine widely available, commercial produced kale cultivars grown in controlled growth environments under a natural photoperiod. These growth conditions, combined with multi-omics analyses obtained at end-of-day (ED)/zeitgeber 11 (ZT11), and end-of-night (EN)/zeitgeber 23 (ZT23) time-points, provides critical new insights into how diverse kale cultivars coordinate diel molecular events, while simultaneously generating a proteome resource for further targeted experimentation. Through the development of this resource we create a foundation for uncovering the key proteins and cell processes underpinning critically important growth and development traits in kale, while also revealing the nutritional content and diel metabolic landscape of nine diverse kale cultivars.

Results

Diversity in kale growth and morphology under horticultural LED light conditions

To compare the growth of nine publicly available and commercially grown kale cultivars (Table 1), we utilized spectral LED lighting conditions that can be implemented in LED driven horticultural growth systems (Supplemental Figure 1A). In addition, we further implemented twilight conditions at ED and EN to mimic a more natural growth environment (Figure 1A; Supplemental Figure 1B). We employed these parameters in order to comparatively evaluate the growth of all nine cultivars in a controlled growth environment setting that represents conditions comparable to those in future-forward vertical farming and horticultural facilities (Figure 1A; Supplemental Figure 1B). These conditions successfully grew all nine kale cultivars, with each

10.3389/fpls.2023.1170448

TABLE 1 Name and classification of kale cultivars used in the study.

Species	Convariety	Variety	Cultivars	Types	Paper Abbreviation
Brassica oleracea	*convar. Acephala*	*var. sabellica*	*cv.* Winterbor	Curly Kale	K2
			cv. Dwarf curled Scotch		K3
			cv. Darkibor		K7
			cv. Starbor		K8
			cv. Scarlet		K9
		var. palmifolia	*cv.* Lacinato	Italian Kale	K4
		var. palmifolia x var. sabellica (Lacinato x Redbor)	*cv.* Rainbow Lacinato	Hybrids	K6
Brassica napus (oleracea x rapa)	*convar. Pabularia*	*var. pabularia*	*cv.* Red Russian (Note: possibility = Siberian Kale x Brassica nigra)	Russian and Siberian Kale	K5
		var. pabularia (Siberian x RedRussian)	*cv.* Red Ursa	Hybrids	K10

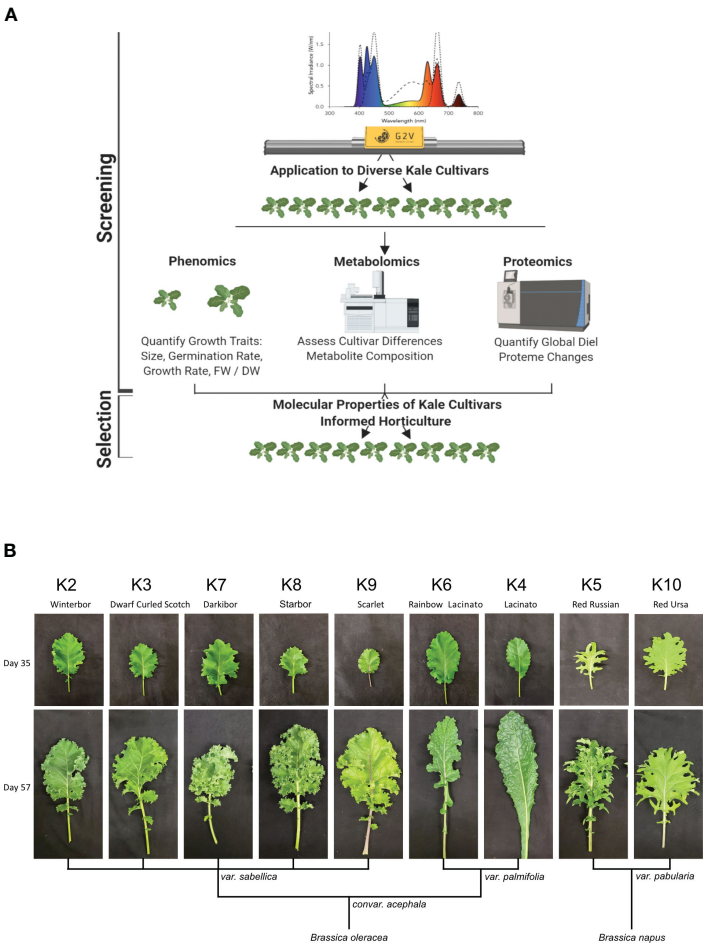

FIGURE 1
Experimental design and kale genetics phenotype. **(A)** Experimental workflow schematic. **(B)** Classification of kale cultivars based on leaf morphology and species.

cultivar presenting unique patterns of leaf size, shape and lobation consistent with previously observed morphologies. However, the leaf reddening typically observed in *B. napus* var. *pabularia* cultivars and the red *B. oleracea* var. *sabellica* 'Scarlet' (Figure 1B; Carvalho and Folta, 2014; Waterland et al., 2019) was not observed. The *B. oleracea* var. *sabellica* cultivars Starbor (K8), Darkibor (K7), Winterbor (K2), Dwarf Curled Scotch (K3) and Scarlet (K9) presented an oval shaped, curly leaf phenotype, while *B. napus* var. *pabularia* cultivars (Red Russian (K5) and Red Ursa (K10) have a notably pronounced, serrated leaf morphology. Alternatively, the Italian cultivars *B. oleracea* var. *palmifolia* (Lacinato and Rainbow Lacinato) present a spear-like leaf phenotype (long and narrow), with a rough surface and darker green coloration relative to the other kale cultivars (Figure 1B). These leaf traits along with leaf size are correlated with each cultivar's origins in Northern Europe, Russia and Italy, respectively (Table 1; Supplemental Figure 2). Lastly, we monitored leaf area over-time using a combination of time-course RGB imaging and PlantCV (https://plantcv.readthedocs.io/), which revealed kale cultivars to differ in their growth rates (Supplemental Figure 2). K10 and K2 varieties demonstrated the largest overall plant area, reaching an area of 13.4 to 12.6 cm^2 at 24 days post-imbibition, while K8 and K5 exhibited the slowest growth rate reaching both a plant area of 8 cm^2 at 24 days post-imbibition (Supplemental Figure 2). We also found that fresh weight (FW) is correlated with leaf area results, with K10 and K2 having the highest weight average of ~ 4 g and K8 and K5 the lowest, with an average of 1 g and 0.8 g, respectively.

To better characterize each cultivars physiological responses, we next measured relative chlorophyll content or Special Products Analysis Division (SPAD) and a variety of photosynthetic parameters (Phi2, PhiNO, PhiNPQ, LEF, ECSt, gH+ and vH+) using the PhotosynQ platform and the handheld MultispeQ device (Kuhlgert et al., 2016). Across the cultivars, relative chlorophyll amount was not significantly different except for the var. *palmifolia* cultivars K4 and K6, where SPAD was significantly higher (Supplemental Figure 2). This is consistent with the darker phenotype of the two var. *palmifolia* cultivars (Figure 1). Phi2, which measures photosystem II quantum yield, was only significantly higher in K5 compared to K10, while exhibiting no significant differences amongst other cultivars. Alternatively, PhiNO, which is a measurement of the electrons lost to non-regulated processes that can result in cellular damage, was significantly higher in K10, demonstrating that while K10 possesses one of the largest leaf areas, it is less effective at harvesting light energy. Interestingly, we find that linear electron flow (LEF), which estimates photosynthesis, exhibits a trend inversely proportional to FW, with large area cultivars possessing lower LEF and small cultivars possessing higher LEF. However, significant differences were only observed between cultivars K6 and K2.

Lastly, we estimated the energy generating capacity of each cultivar by measuring a series of parameters relating to ATP generation (Supplemental Figure 2). This included: ECSt, gH+ and vH+. ECSt, which describes the magnitude of the electrochromic shift, was higher in the K2 cultivar compared to K4, K8 and K9, suggesting better ATP production for increased growth outcomes while also aligning with their increased growth rate relative to other kale cultivars. Conversely, thylakoid proton conductivity (gH+), which describes steady state proton flux, was highest in the smallest cultivar K9, suggesting more efficient energy generation. However, despite differences in the ECSt and gH+, the initial rate of proton flux through ATP synthase (vH+) was constant across the cultivars. Taken together, these results indicate that photosynthetic parameters LEF and ECSt define important physiological differences in kale cultivars that likely contribute to observed differences in morphology and biomass.

Diel metabolome analysis

As previous research in the related *Brassicaceae* Arabidopsis has demonstrated the importance of the ED and EN photoperiod transitions (Zeitgeber; ZT11-12 and ZT23-0; respectively) at the molecular-level (Uhrig et al., 2019; Krahmer et al., 2022), we next analyzed the metabolite content of each cultivar at ED (ZT11) and EN (ZT23). Aligning with other diel metabolite studies from the related species Arabidopsis (Flis et al., 2019; Cervela-Cardona et al., 2021) we quantified diel changes in 40 key metabolites across all nine cultivars, which can be grouped into 8 molecule classes: amino acids (12), organic acids (7), sugars (6), fatty acids (4), sterols (1), phenylpropanoid pathway metabolites (4) and vitamins (3) (Figure 2; Supplemental Figure 3; Supplemental Data 1). Hierarchical clustering using Euclidian distance further revealed that based on these 40 metabolites, the kale cultivars analyzed form 2 distinct groups based on their patterns of diel metabolite level fluctuations (Figure 2; Supplemental Data 1). This included a group consisting of

Darkibor (K7), Starbor (K8), Red Russian (K5) and Red Ursa (10), which form Group I and Winterbor (K2), Dwarf Curled Scotch (K3), Scarlet (K9), Rainbow Lacinato (K6) and Lacinato (K4), which form Group II. This grouping now allows us to establish additional kale relationships at the molecular-level (Supplemental Figure 3). Interestingly, Group I kale demonstrate more extensive leaf lobation and serration relative to their Group II counterparts, suggesting a correlation between leaf phenotype and diel metabolite changes. Further, hierarchical clustering analysis revealed two clusters of metabolites, whose relative change in diel abundance seem to be core to the differences between Group I and Group II (Figure 2). This includes: carbohydrates xylose, glucose and fructose; and amino acids aspartic acid, serine and iso-leucine, along with shikimate and α-linolenic acid (Figure 2). Of the compounds that kale produces in larger quantities that are of direct nutritional importance, we detected vitamins niacin (vitamin B3), ascorbic acid (vitamin C) and phytol (vitamin E precursor) in addition to α-linolenic acid (omega-3 fatty acid), with the majority of the kale cultivars possessing increased amounts of these vitamins at EN (Figure 2). Within Group II kale, we also see a sub-cluster consisting of K6 and K9 cultivars, which is largely defined by increased abundance of glyceric acid and glycine at ED.

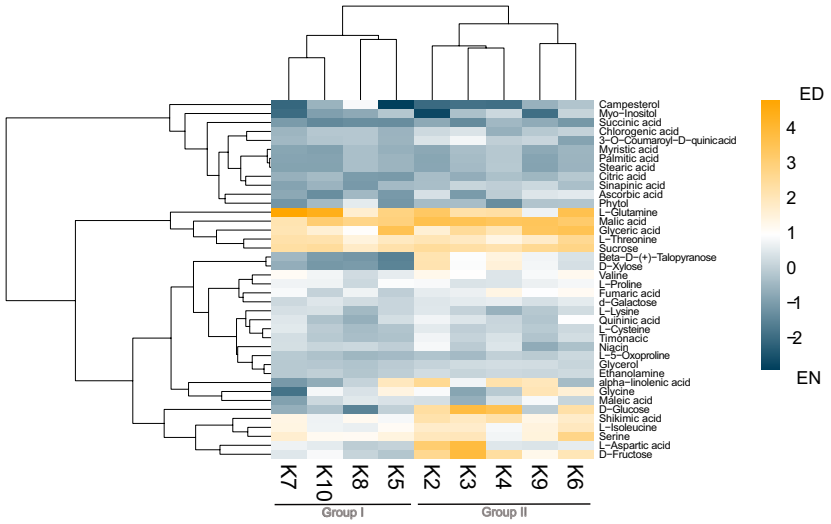

FIGURE 2
Diel changes in the kale metabolic landscape. Eucledian distance clustered heatmap of relative diel metabolite changes with each kale cultivar reveals two clusters of kale based on diel metabolic changes. Scale represents Log2 fold-change (FC); n=4 biological replicates.

Diel proteome analysis

To further contextualize Group I and Group II kale, we next performed quantitative proteomic analysis using an advanced data independent acquisition (DIA) workflow called BoxCarDIA which is aimed at better analyzing high complexity, high dynamic range plant samples (Mehta et al., 2022). With the kale analyzed in this study representing a diverse assemblage of cultivars without specifically sequenced genomes, we performed our quantitative proteomic searches using the *B. oleracea var oleracea* proteome. Here, we were able to quantify a total of 2124 protein groups across all nine cultivars (Supplemental Data 2). Of these, a total of 1734 protein groups exhibited a significant change in diel abundance (Bonferonni corrected $p\text{-value} \leq 0.05$ and $\text{Log2FC} \geq 0.58$) in at least one of the nine kale cultivars examined (Supplemental Data 2). Comparative quantification of the significantly changing proteins at ED and EN supported our metabolite-defined Group I and Group II clusters, with Group I kale possessing more proteins with a significant change in abundance at EN and Group II kale generally possessing more proteins changing at ED (Figure 3A).

Next, we analyzed all significantly changing proteins for enrichment of Gene Ontology (GO) terms relating to biological processes and molecular functions (BH corrected $p\text{-value} \leq 0.05$). Here we found a significant enrichment of biological processes core to plant growth and development. These include significant enrichment of protein translation (GO0006412; GO:0006414), photosynthesis (GO:0009765; GO:0015979), cell redox homeostasis (GO:0045454), glycine metabolism (GO:0019464), lipid transport (GO:0006869) and primary metabolism (GO:0006096), amongst others (Figure 3B). Underpinning these biological processes was the significant enrichment of molecular functions related to translation initiation (GO:0003743) and elongation (GO:0003746), ribosome composition (GO:0003735), chlorophyll binding (GO:0016168) and oxidoreductase activity (GO:0016620), amongst other terms, which relate to protein translation, photosynthesis and cell redox homeostasis, respectively (Figure 3C).

To further elucidate when and where these protein-level changes differentially occur between Group I and II kale, and to increase our resolution of enriched biological processes, we performed an association network analysis using the knowledge database STRING-DB (https://string-db.org/). With *B. oleracea var oleracea* not possessing a STRING-DB dataset, we first identified orthologs from Arabidopsis for all significantly changing proteins using UniProt (https://www.uniprot.org/). Correspondingly, we identified orthologous Arabidopsis gene identifiers for 80.4% (1395/1734) of the significantly changing proteins originally quantified (Supplemental Data 3). Using a highly stringent STRING-DB score of ≥ 0.9, we then mapped an association network for Group I and Group II kale. This revealed diel abundance changes in proteins related to RNA splicing, both cytosolic and plastidial translation, chlorophyll biosynthesis, chaperones, mitochondrial respiration and elements of carbon metabolism, with Group I exhibiting specific changes in the proteasome, protein secretion, fatty acid biosynthesis and methionine metabolism, while Group II maintained specific changes in the phagosome (Figure 4). STRING-DB analyses were further contextualized by subcellular localization data to elucidate where ED and EN changes manifest within the subcellular landscape (Figure 5). Group I predominantly exhibited changes at EN relating to proteins localized to the plastid, cytosol, mitochondria and extracellular compartments, while Group II exhibited most changes in similar compartments (plastid, cytosol and mitochondria), but at ED (Figure 5).

Lastly, using orthologous Arabidopsis gene identifiers for the significantly changing proteomes of Group I and II kale, we performed a metabolic pathway enrichment analysis using the Plant Metabolic Network (PMN; https://plantcyc.org/;

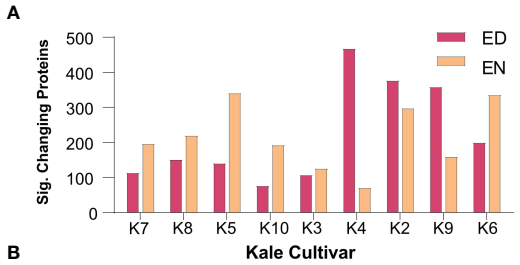

B

GO Term	Description	Fold Enrichment	*pvalue*	BH FDR
GO:0006412	translation	2.867301442	6.94050992	9.71E-20
GO:0006457	protein folding	3.532226149	2.76203966	1.28E-09
GO:0009735	response to cytokinin	5.833630563	1.13314448	2.60E-06
GO:0015979	photosynthesis	3.554868624	1.27478754	6.26E-04
GO:0042026	protein refolding	8.294693457	0.49575071	0.004121373
GO:0006414	translational elongation	8.294693457	0.49575071	0.004121373
GO:0009765	photosynthesis, light harvesting	5.078383749	0.7082153	0.004121373
GO:0019464	glycine decarboxylation via glycine cleavage system	11.84956208	0.35410765	0.013029916
GO:0018298	protein-chromophore linkage	4.308931666	0.7082153	0.013029916
GO:0051017	actin filament bundle assembly	7.756076999	0.42492918	0.01946313
GO:0045454	cell redox homeostasis	2.0313535	1.84135977	0.029462255
GO:0006869	lipid transport	3.646019102	0.7082153	0.035279163
GO:0009658	chloroplast organization	4.550231839	0.56657224	0.035279163
GO:0006096	glycolytic process	3.763978544	0.63739377	0.051183229

C

GO Term	Description	Fold Enrichment	*pvalue*	BH FDR
GO:0003735	structural constituent of ribosome	3.613022412	7.29461756	1.73E-28
GO:0000166	nucleotide binding	3.376817465	4.67422096	4.15E-16
GO:0003676	nucleic acid binding	2.303738703	5.31161473	1.78E-09
GO:0003723	RNA binding	2.180256549	3.11614731	1.49E-04
GO:0003743	translation initiation factor activity	3.972807771	1.20396601	2.17E-04
GO:0003746	translation elongation factor activity	5.986176415	0.63739377	0.002948514
GO:0016168	chlorophyll binding	5.240423798	0.7082153	0.002948514
GO:0009055	electron carrier activity	2.391640223	1.84135977	0.002948514
GO:0005509	calcium ion binding	2.064883407	2.26628895	0.005620431
GO:0016620	oxidoreductase activity	6.371252091	0.49575071	0.014811511
GO:0003755	peptidyl-prolyl cis-trans isomerase activity	4.446873908	0.63739377	0.018201474
GO:0004332	fructose-bisphosphate aldolase activity	9.607443629	0.35410765	0.026338488

FIGURE 3
Diel changes in the kale proteome. Sampling diverse kale genetics provides a robust depiction of diel plant cell regulation in kale (n=4). **(A)** Number of proteins exhibiting diel changes in protein abundance within each kale cultivar examined at ED and EN. **(B)** Gene Ontology (GO) enrichment analysis of biological processes and **(C)** molecular function among all significantly changing proteins (Bonferonni corrected q-value ≤ 0.05; Log2FC ≥ 0.58 or ≤ -0.58).

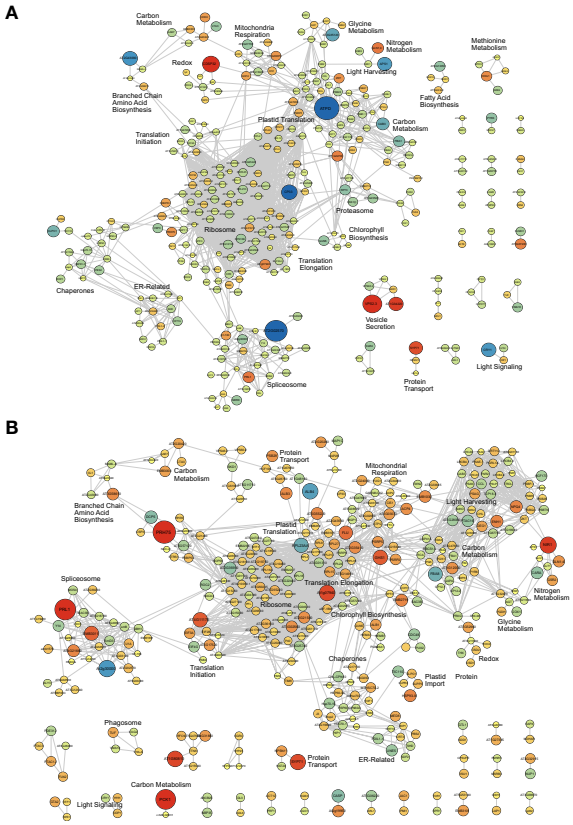

FIGURE 4
Association network analysis of the diel kale proteome. Proteins exhibiting significant diel changes in abundance within Group I **(A)** and Group II **(B)** kale, respectively, were subjected to association network analysis (https://string-db.org/). To maximize the analysis, Brassica oleracea var. oleracea gene identifiers were converted to Arabidopsis thaliana ortholog gene identifiers using UniProt (https://www.uniprot.org/). Proteins exhibiting significant changes in abundance are defined by a Bonferonni corrected q-value ≤ 0.05 and a Log2FC ≥ 0.58 or 5 -0.58). Up- (red) and down- (blue) regulated proteins are shown, with node size related to magnitude of Log2FC.

Supplemental Data 6). This revealed the enrichment of several pathways (Fisher's Exact Test < 0.01) directly related to the metabolites measured by our GC-MS analyses that differ between Group I and II kale, such as multiple pathways related to amino acid and sugar metabolism (Supplemental Data 6). In Group I kale we find an enrichment of serine biosynthesis, which is consistent with our metabolite findings (Figure 2). Specifically, we see serine pathway enzymes (e.g. SERINE HYDROXYMETHYLTRANSFERASE 1; SHM1) exhibiting an average Log2FC change in abundance of 1.45 at ED (Supplemental Data 2, 6). Amongst Group II kale, we see an enrichment of carbohydrate/sugar degradation, which aligns with our observed increase in glucose, fructose and xylose at ED. Here, we find significant increases in the abundance of STARCH-EXCESS 4 (SEX4; Log2FC = 0.68), which degrades starch to affect glucose-levels and FRUCTOKINASE-LIKE 2 (FLN2; Log2FC = 1.22), which phosphorylates fructose to create fructose 6-phosphate, at EN, likely contributing to increased pools of glucose and fructose during the day. We also see an increase of xylan degrading enzymes BETA-XYLOSIDASE 6 (BXL6; Avg Log2FC = 0.162) and ALPHA-XYLOSIDASE 1 (XYL1; Log2FC =0.70) that likely contribute the observed increase in Group II xylose at ED. Lastly, we also find an enrichment of multiple overlapping pathways between Group I and II kale, suggesting that while the timing of amino acid and core carbohydrate metabolism at our sampled ED and EN time-points may differ, there may be additional pathways that have group-specific diel changes at alternative time-points.

Discussion

Diverse kale cultivars form two groups based on phenotypic and metabolic signatures

As the functional components of all biological systems and the defining elements of nutrition, the proteome and metabolome represent a reliable means by which to elucidate differences between diverse, but related plant genetics. In the case of kale, it is the underlying molecular differences between cultivars that offer unique opportunities for targeted breeding and growth manipulation to enhance nutrition and biomass production. To

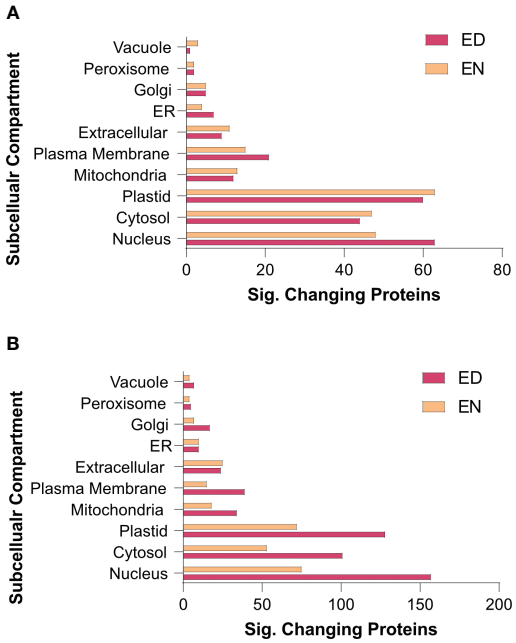

FIGURE 5
Subcellular localization analysis of the kale diel proteome. Subcellular localization analysis of Group I **(A)** and II **(B)** kale proteins exhibiting a significant change in diel abundance, respectively (https://suba.live/). To maximize this analysis, *B oleracea* var. *oleracea* gene identifiers were converted to *Arabidopsis* ortholog gene identifiers using UniProt (https://www.uniprot.org/). Proteins exhibiting significant changes in abundance are defined by a Bonferonni corrected q-value ≤ 0.05 and a Log2FC ≥ 0.58 or ≤ -0.58).

date, differences between kale cultivars has been largely defined phenotypically through leaf morphologies such as coloration, size, shape, lobation and serration (Arias et al., 2021). A few studies have complemented this with transcriptomic analyses of individual cultivars (Chiu et al., 2018; Jeon et al., 2018; Jin et al., 2018; Arias et al., 2021), while others have undertaken metabolomics analyses (Chiu et al., 2018; Jeon et al., 2018). This has predominantly involved targeted metabolomics, examining single kale cultivars for changes in pigmentation (Redbor; var. *sabellica*; (Klopsch et al., 2019), flavonols (Winterbor; var. *sabellica*; (Neugart et al., 2014; Neugart et al., 2016; Neugart and Bumke-Vogt, 2021) and fatty acids (Black Cabbage; *convar. acephala*; (Ayaz et al., 2006), with few studies having pursued global metabolite profiling of an individual kale cultivar (Nemzer et al., 2021). Correspondingly, our systems-level analysis of the leaf proteome and metabolome from nine kale cultivars in the same study using non-targeted GC-metabolomic and LC-proteomic mass spectrometry (MS), respectively, represents a substantial advancement in resolving the broader molecular landscape of kale for future targeted investigations.

Under our growth conditions no red/purple pigmentation in any kale cultivar was observed despite some of the cultivars examined (K9, K5 and K10) being known to have elevated anthocyanin production (Waterland et al., 2019). As a goal of our study was to define the diel molecular landscape of kale across diverse kale cultivars using near-sunlight conditions, our finding of no observable anthocyanin production was very informative (Figure 1; Supplemental Figure 2). It suggests that LED light recipes deployed in controlled growth environments can be utilized to drive substantially different growth outcomes in the same kale variety. This aligns with previous studies, which revealed the application of UV light enhances the profile of flavonoids in kale (Neugart et al., 2014; Neugart and Bumke-Vogt, 2021). Flavonoids are important molecule class in kale, as they represent the molecular precursors for the red/purple coloration some kale cultivars exhibit via anthocyanin (Liu et al., 2021).

Unexpectedly, our analysis of the diel metabolome landscape across nine kale cultivars revealed two groups based on their metabolite signatures. Group I is comprised of both *B. oleracea* (K7 and K8) and *B. napus* (K5 and K10) cultivars, despite notable differences in ploidy between *B. oleracea* (diploid) and *B. napus* (polyploidy) (Gao et al., 2022). This suggests that higher level differences in genomic architecture do not seem to determine baseline growth traits in kale. Group I kale also maintained similarities in leaf lobation architecture, exhibiting a jagged and pronounced lobation morphology relative to the kale cultivars of Group II. Conversely, Group II kale consisted entirely of *B. oleracea* cultivars, which have substantially different and more variable lobation morphologies. The var. *palmifolia* cultivars K6 and K4, have a narrow leaf shape and almost no leaf lobation, while the var. *sabellica* cultivars K2, K3 and K9 have a round and wavy leaf shape with more leaf lobation. No specific photosynthesis or ATP production measurements were found to correlate with these metabolite-based groupings, likely due to the higher order nature of those processes relative to diel metabolite changes; however, Group II kale did possess more light harvesting/photosynthesis and mitochondrial respiration proteins exhibiting a diel change in their abundance relative to Group I. Using un-targeted metabolomics to define groups within a complex species has also proven successful with other crops (*Cucumis melo*; (Moing et al., 2020). Here, a variable alignment between phylogeny and the metabolome was found that parallels our findings in kale. Taken together, our combined phenotypic and diel-metabolomic definition of nine kale cultivars suggests that metabolomic fingerprinting provides a more contextualized understanding of kale cultivars, however, future studies could consider more wide-ranging, untargeted LC-based metabolomics analyses. Overall, our findings provide an initial resource for future research of this leafy-green super food, in addition to offering actionable information for vertical farming and horticultural kale producers.

Underlying metabolic differences between kale cultivars offers opportunities for production systems

Upon comparing the diel metabolite profiles of our nine kale cultivars, we found a series of core compounds that are critical pre-requisites for the production of nutritionally valued specialized metabolites. Further, many of these metabolomic differences seemed to define Group I and II kale. These compounds include: carbohydrates (xylose, glucose and fructose), amino acids (serine, glycine, aspartic acid and iso-leucine) as well as shikimic acid and

α-linolenic acid (Figure 2; Supplemental Data 1). This analysis successfully defined the molecular potential of each kale cultivar, while also providing information for time-of-day kale harvesting in order to maximize its nutritional content. With the circadian clock and diel plant cell regulation highlighted as a critical consideration for next-generation agriculture [e.g. chronoculture (Steed et al., 2021)], it is important that researchers and vertical farming/horticulture producers have reliable data resources generated using precision LED light systems.

Carbohydrates – Carbohydrates represent an important energy source for both plants and humans. Sugars, such as glucose and fructose, are a particularly important component of kale taste, which plays an important role in cultivar attractiveness, as kale is generally characterized as having a bitter and earthy flavor profile (Barker et al., 2022). Like other plants, kale possesses peak sucrose levels at ED, which in combination with transient leaf starch degradation, is vital for driving plant growth at night. At night, leaf starch is degraded to produce glucose, while sucrose is degraded to produce both glucose and fructose (Kim et al., 2017). Despite relatively consistent diel sucrose levels observed across both kale groups, we find a distinct diel pattern of glucose and fructose abundance between Group I and II kale (Figure 2; Supplemental Figure 3; Supplemental Data 1). Group I kale possess more fructose at EN, suggesting they may have better cold-temperature tolerance as fructose enhances cold-induced oxidative stress adaptation by preserving homeostasis under low temperatures (Bogdanovic et al., 2008). This diel difference could also be explained by cultivars originating from northern latitudes (e.g. K5 and K10). Further, fructose can be involved in vitamin C biosynthesis through its conversion to fructose-6-phosphate by fructokinase, which can also aid in cold tolerance (Akram et al., 2017), while also being an essential vitamin for human consumption. Diel changes in vitamin C leading to an accumulation at EN may offer to ease the transition to a high light environment come morning given its antioxidant properties (Paciolla et al., 2019). There is also a positive relationship between sucrose metabolism and anthocyanin production (Shi et al., 2014), which aligns with typically red cultivars K5 and K10 and their enhanced diel accumulation of fructose and glucose at EN. Alternatively, typically green cultivars K4 and K6 of Group II kale possess maximal fructose levels at ED, which aligns with our pathway enrichment analysis and peak abundance changes in key metabolic enzymes related to carbohydrate degradation (Supplemental Data 2, 6).

Additional carbohydrates xylose, myo-inositol and galactose were also present in different quantities across cultivars and throughout the day. Myo-inositol is involved in an array of biological processes such as being a precursor of inositol phosphates (Ips), hormones (auxin), translocation of mRNA into the cytosol, membrane biogenesis, light response germination and abiotic stress response (Munnik et al., 1998). Alternatively, xylose is a major component of the cell wall hemicellulose xylan, which provides plant cell resistance against enzymatic digestion and represents up to 35% of some wood compositions (Rennie and Scheller, 2014). Xylose is derived from UDP-Glucose and is transported to Golgi where xylan is produced, which aligns with the large number of secretion related proteins (e.g. ER, Golgi and extracellular) we see significantly changing in both Group I and II kale. It also specifically aligns with our pathway enrichment analysis for Group II kale, where we find increased abundance of xylan degrading enzymes that would increase the amount of xylose available during the day (Supplemental Data 2, 6). Xylose functions as a dietary fiber with prebiotic properties (Thavarajah et al., 2016). With Group I and II kale having contrasting diel xylose levels, the beneficial properties of xylose may offer value-added properties to a cultivar based on time-of-day harvesting.

Amino acids – Our analysis of the diel metabolome found that glycine, serine and aspartic acid have group specific differences in diel abundance. Both serine and glycine predominantly accumulated at EN and ED in Group I and II kale, respectively. Of these amino acids, serine in particular, functions as a key substrate for the biosynthesis of molecules critical for plant growth, including: amino acids glycine, methionine and cysteine (an essential amino acid for human nutrition), nitrogenous bases, proteins, phospholipids and sphingolipids (Stein and Granot, 2019). Specifically, our pathway analysis found an enrichment of serine biosynthesis in Group I kale, with our proteome data indicating that this occurs at ED (Supplemental Data 2, 6). Additionally, we find group specific differences in aspartic acid levels, which is also a precursor for several other amino acids, including: lysine, methionine, threonine and isoleucine (Han et al., 2021), with lysine representing an essential amino acid, whose content in plants is a key nutritional trait for crop improvement (Galili and Amir, 2013). Amongst the kale cultivars examined however, we see lysine consistently produced at EN while we see iso-leucine demonstrating group specific diel abundance changes. Iso-leucine is one of three branched chain amino acids (BCAA; e.g. leucine, isoleucine and valine), but is the only BCAA not built from pyruvate (Joshi et al., 2010). With the BCAA isoleucine an integral to plant defense as a conjugate of jasmonic acid (Armenta-Medina et al., 2021) and being up-regulated in response to drought and cold (Joshi et al., 2010), our data suggest that Group I and II kale may have differences in their stress mitigation capacity.

Shikimic acid – Shikimic acid is a precursor of the essential aromatic amino acids tyrosine, phenylalanine and tryptophan and therefore is an important precursor for the phenylpropanoid biosynthetic pathway, which is responsible for the production of a large number of nutritionally valued specialized metabolites (Dong and Lin, 2021). Production of shikimic acid can consume upwards of 30% of the fixed carbon, feeding the production of vitamins K1, B3 (folate), E (tocopherols), in addition to flavonoids, anthocyanins and lignin (Tohge et al., 2013). The shikimic acid pathway is also involved in the color patterning seen in ornamental kale through modulation of anthocyanin content, which is a key trait in kale as a source of antioxidants (Liu et al., 2021).

α-linolenic acid – Kale is known to be rich in α-linolenic acid, however, the differences in abundance between cultivars and the diel production landscape of α-linolenic acid have not previously been assessed. α-linolenic acid is a polyunsaturated Omega 3 fatty acid, which is an essential component of a healthy diet (Nemzer et al., 2021), as omega 3 fatty acids are known to decrease the risk of heart disease and lower the blood pressure (Shahidi and Ambigaipalan, 2018). Importantly, α-linolenic acid also forms the

basis of cell membrane components as a precursor of phosphoglycerolipids, cutin and waxes (He and Ding, 2020). With α-linolenic acid contributing broadly to many of the important nutritional properties of kale and our results demonstrating it maintains diel changes in abundance, along with differences in abundance between cultivars, α-linolenic acid offers an array of opportunities for further development of cultivar specific light recipes to maximize its production.

Differences in the diel proteomes of Group I and II kale indicate they are defined by core elements of plant cell regulation

Elucidating the specific molecular components that underpin the observed metabolomic changes of Group I and II kale revealed a number of plant cell processes that are diel regulated at the protein-level. In particular, we find diel proteome changes across multiple subcellular compartments related to metabolism, RNA processing, protein translation and light harvesting. With diel biology/the circadian clock critical for timing the transitions from day-to-night and night-to-day, understanding where within the cellular environment [e.g. subcellular compartment(s)] molecular changes manifest, can help further resolve each kale cultivars potential agronomic viability from a chronoculture perspective (Steed et al., 2021). From a metabolic perspective, we find diel changes in: carbon, nitrogen, glycine, methionine, BCAA and fatty acid metabolism (Figure 2), which we also see enriched at the pathway level (Supplemental Data 6), while for RNA processing and protein translation, we find: mRNA splicing, cytosolic and plastidial protein translation along with a number of chaperones to exhibit significant diel changes. We also observed differences involving numerous light harvesting and signaling proteins, along with differences in chlorophyll biosynthetic enzymes, which may also be directly related to Group specific productivity differences. At the highest level, our quantitative proteomic analysis resolved Group I kale cultivars to possess significant changes in their diel proteome at EN, while Group II kale exhibit more significant proteome-level changes ED (Figure 3). We also note that many significantly changing metabolic proteins are directly connected to observed diel metabolome changes, reinforcing our multi-omics approach (Supplemental Data 6). Further, significant changes in numerous other, non-metabolic proteins central to proper plant cell regulation demonstrate how quantitative proteome analysis allows us to map diel molecular landscape changes in order to identify how kale breeders and producers can better realize each cultivars genetic potential.

Metabolism – Significant changes in the diel proteome related to plant metabolism were wide-ranging, aligning with the metabolite-determined kale groupings. Enzymes involved in carbon and nitrogen metabolism exhibiting a significant diel change in abundance demonstrated coherent time-of-day changes between both kale groups, consistent with their central roles in plant growth and development. Conversely, amino acid metabolic enzymes aligned with the metabolite-defined kale groups, specifically BCAA-related enzymes and glycine metabolic enzymes, likely relating to the specialized metabolites produced by kale that are derived from these amino acids.

From a carbon metabolism perspective, diel changes centered around two protein clusters comprised of mitochondrial enzymes isocitrate dehydrogenase (cICDH), ATP citrate lyase and components of the pyruvate dehydrogenase complex, along with key primary metabolic enzymes fructose-bisphosphate aldolase (FBA), glyceraldehyde 3-phosphate (GAPA) and phosphoglycerate kinase (PGK). With acetyl-CoA representing a critical metabolite involved in multiple biosynthetic pathways, including fatty acid biosynthesis (Xing and Poirier, 2012), it is perhaps not surprising that cICDH and ATP citrate lyase enzymes exhibit consistent diel abundance changes in both Group I and II kale (Figure 4; Supplemental Data 2). Similarly, FBA, GAPA and PGK enzymes consistently exhibited significant diel abundance changes across both Group I and II, offering a consistent benchmark for our systems-level proteome analysis (Supplemental Figure 4A). Intriguingly, different isoforms of PGK and FBA were found to possess significant changes in diel abundance between Group I and II kale, whose activity may be directly related to diel differences in Group I and Group II fructose levels though changes in fructose 1,6-bisphosphate. This possibility is further reinforced by the enrichment of multiple sugar related metabolic pathways amongst both Group I and II kale (Supplemental Data 6). In Arabidopsis, the three encoded FBAs were found to have essential roles in plant metabolism, but with tissue specific expression patterns (Carrera et al., 2021). Here however, it seems that Group I and II kale each utilize a different subset of FBA isozymes, as we analyzed the same leaf tissues across cultivars. Unlike Arabidopsis, the polyploid *B. napus* has been shown to possess twenty-two FBAs, which possess diverse developmental expression patterns across multiple cellular compartments (Zhao et al., 2019). Further, it seems that despite fructose and glucose representing two of the group defining metabolites in our study, very few protein groups related to the generation of fructose and glucose such as starch degradation enzymes, sucrose synthase or invertase, were found to be significantly changing in our proteomics data (Figure 4; Supplemental Data 2). This perhaps indicates that changes in these enzymes, such as their activity are driven by other regulatory mechanisms such as reversible protein phosphorylation, rather than changes in abundance (Hardin et al., 2004).

We also quantified changes in nitrogen assimilating enzymes in both Group I and II kale. Group I kale cultivars possess substantially larger diel changes in nitrite reductase (NiR) levels at ED relative to Group II, while glutamine synthetase isoform 1,4 (GLN1,4), which converts glutamate to glutamine as part of nitrogen assimilation for transport from roots to shoots, exhibited a consistent and significant change in abundance at ED in both Group I and II kale. This aligns with both our metabolite data (Figure 2; Supplemental Data 1) and pathway enrichment analysis (Supplemental Data 6), which finds glutamine levels to peak in nearly all nine kale cultivars at ED. In the model *Brassicaceae* Arabidopsis, it is well known that nitrogen metabolism is a diel regulated process (Flis et al., 2019), with peak transcript and protein abundance of nitrate reductase enzymes occurring early in the day, however here, it seems that the precise time-of-day coordination of these events differs between kale cultivars (Supplemental Figure 4B).

Directly related to both carbon and nitrogen metabolism, our proteomics data and pathway enrichment analysis also resolved extensive amino acid metabolism changes (Figure 4; Supplemental Data 2, 6). In particular, we find significant Group I and II differences in the diel abundance of enzymes related to glycine, serine and BCAA (e.g. iso-leucine) metabolism (Schulze et al., 2016). We also find time-of-day differences in iso-leucine production, which is produced down-stream of aspartate and possesses group-specific time-of-day production differences. Here, both our pathway (Supplemental Data 6) and proteomics (Supplemental Data 2) analyses support the diel differences in BCAA levels (e.g. isoleucine and valine) observed between Group I and II, with BCAA super-pathway enzymes possessing average ED (Log2FC = 0.63) and EN (Log2FC = 0.42) abundance differences, respectively. Interestingly, despite aspartate fueling lysine and methionine production, and our measurements of aspartate and lysine providing no indications of group specific responses (Figure 2; Supplemental Data 1), we find Group I kale to specifically possess a significant change in methionine metabolic enzymes. Collectively, these aligned diel differences in both the proteome and metabolome relating to amino acids makes a case for genetics-based time-of-day harvesting of kale for maximal nutritional content.

mRNA Processing & Protein Translation – RNA splicing and protein translation represent two cellular processes carried out by multi-subunit protein complexes; the spliceosome and the ribosome, respectively. However, much remains to be resolved as to how each of these complexes are regulated in plants at the protein level. Previous diel proteome analyses have found both the spliceosome and ribosome to be dynamically regulated at the protein-level by changes in both abundance and phosphorylation (Uhrig et al., 2021). However, resolution of species-specific differences in diel abundance has not previously been resolved. Here we see Group I and II kale defined by smaller abundance changes in mRNA processing and protein translation machinery at EN in Group I kale, coupled with larger abundance changes at ED in Group II kale. Correspondingly, a large abundance of chaperone proteins changing in a similar pattern at the same time-points is observed, likely aiding in effective protein production. Surprisingly, we also see a large abundance of plastidial translational machinery in both Group I and II kale, which parallel the diel changes in abundance found in their cytosolic counterparts, suggesting concerted coordination of global protein production in each kale group. Currently our understanding of diel changes in mRNA splicing and protein translation have largely been defined by transcriptomic sequencing technologies. In particular, use of polysome loading or RiboSeq as a proxy for protein translation, which in Arabidopsis is suggested to negatively correlate with biomass (Ishihara et al., 2017). Similarly, RNAseq profiling of Arabidopsis over a 24 h photoperiod has found diel changes in mRNA spliceforms (Romanowski et al., 2020), however, in both areas of research, direct diel assessment of spliceosome or ribosome complex composition and regulation at the protein-level has remained undefined. In light of the work performed in the related *Brassicaceae* Arabidopsis, our findings here suggest that there are systemic differences between the kale groups in the timing of growth as it relates to protein translation that could be utilized to enhance the productivity kale through the precise adjustment of growth conditions.

Light Harvesting and Signaling – In both Group I and II kale we see extensive diel changes in the light harvesting and photosynthetic machinery, with no specific ED or EN changes in either group. The largest changes observed involved the chloroplast ATP synthase delta subunit (ATPD) at EN in Group I kale along with enzymes ENHANCER OF SOS3-1 (ENH1) and NONPHOTOCHEMICAL QUENCHING 4 (NPQ4) at ED in Group II kale. Chloroplast ATP synthase is a critical driver of ATP production in plants in the light, with *Arabidopsis* plants lacking ATPD presenting a lethal phenotype due to the destabilization of the ATP synthase complex (Maiwald et al., 2003). Alternatively, ENH1 is required to main redox balance (Zhu et al., 2007) and NPQ1 is involved in non-photochemical quenching in the presence of excess light energy, which led to increased growth outcomes in tobacco when present in higher abundance (Kromdijk et al., 2016). Interestingly, in both Group I and II kale we also observe a small, but important network of proteins comprised of CRYPTOCHROME 1 (CRY1), ELONGATED HYPOCOTYL 5 HOMOLOG (HYH) and CONSTITUTIVE PHOTOMORPHOGENIC 1 (COP1), with CRY1 more abundant at EN in Group I kale. In response to blue light, CRY1 inhibits the degradation of the HY5 transcription factor by COP1 (Wang et al., 2018). Although there is a more limited understanding of HYH, HY5, an HYH ortholog, is a regulator of light-mediated transcription in plants, controlling a wide range of plant cell processes related to growth and development that are of importance to kale production (Xiao et al., 2022). CRY1 is also connected to the circadian clock through detection of blue light fluence (Somers et al., 1998; Sanchez et al., 2020), indicating potential higher-order regulation of timed-metabolism in Group I versus Group II kale. This has particularly intriguing chronoculture implications for Group I kale production in controlled growth environment settings given its larger diel abundance changes.

Summary

Our integrated, systems-level analysis of nine diverse, commercially produced and readily consumed kale cultivars has substantially advanced our understanding of kale from the phenotypic-level to the underlying molecular-level. In doing this, our dataset reveals new information about the molecular landscapes of these kale cultivars when grown under standardized controlled growth environment conditions, providing new opportunities for vertical farming and/or horticultural growth of kale. Our systems-level analysis has defined diel differences in the molecular landscapes underpinning these diverse kale genetics, elucidating information for time-of-day harvesting considerations to ensure maximal nutritional content. Variations in the diel molecular landscapes of different cultivars or plant accessions have been previously observed in *Arabidopsis* (Rees et al., 2021), tomato (Muller et al., 2016) and soybean (Greenham et al., 2017), with explanations for these differences being related to environmental stimuli and/or geography (seasonal impacts and latitude) (Ruts

et al., 2012; Steppe et al., 2015; Rees et al., 2021). It is also interesting, that many of those differences have been linked to diel plant biology. Here, we observe differences in proteins linked to light perception and the circadian clock (e.g. CRY1), while simultaneously finding group-specific differences in multiple metabolites and pathways connected to diel biology and the circadian clock (Haydon et al., 2013; Cervela-Cardona et al., 2021; Scandola et al., 2022). Overall, our endeavor to define the underlying molecular landscape of diverse, commercially grown kale cultivars opens up new opportunities for horticultural production and targeted research activities moving forward. Further, our results suggest that combined use of plant phenotyping, proteomics and metabolomics represents a powerful approach for characterizing non-model horticultural crops of diverse genetic backgrounds.

Materials and methods

Growth conditions

Nine commercially grown cultivars of kale were purchased from OCS Seeds (Table 1; https://www.oscseeds.com/) and West Coast Seeds (https://www.westcoastseeds.com/) and grown for the study. These included: *B. oleracea* var. *sabellica* cultivars Winterbor (K2), Dwarf Curled Scotch (K3), Darkibor (K7), Starbor (K8), Scarlet (K9), *B. oleracea* var. *palmifolia* cultivars Lacinato (K4), Rainbow Lacinato (K6) and *B. napus* var. *pabularia* cultivars Red Russian (K5) and Red Ursa (K10). Seeds were sterilized in 70% ethanol for 2 min followed by a 70% (v/v) bleach (Chlorox 7.5%) treatment for 7 min and 3 washes with distilled water. The seeds were then grown on ½ MS media containing 1% (w/v) sucrose and 7 g/L of agar at pH 5.8. The seeds were cold treated 3 days at 4°C in the dark and exposed to a 12h light and 12h dark photoperiod consisting of 100 PPFD for a week before being transferred to soil (Sun Gro®, Sunshine Mix® #1). At 29 days post-sterilization, entire plants were collected for GC-MS and LC-MS analysis. Growth chambers were equipped with a programmable Perihelion LED fixture (G2V Optics Inc; https://g2voptics.com/) and lined with Reflectix® to ensure a good light distribution. Kales were grown under a 12h light and 12h dark regimen consisting of 100 PPFD and a temperature of 21°C during the day and 19°C at night. All physiological and phenotypic assessments were performed at ZT6 (mid-day). Physiological measurements were taken using a multispecQ device (PhotosynQ; https://www.photosynq.com/product-page/multispeq-v-2-0).

Metabolite extraction and GC-MS analysis

Metabolite Extraction and Data Acquisition - Metabolite extraction and preparation were performed with modifications as previously described (Liu et al., 2016). Leaf tissue was harvested at ZT23 (end-of-night) and ZT11 (end-of-day) and directly flash frozen in liquid nitrogen (n = 4; each biological replicate consists of a pool of leaf tissue from 3 plants). Sample of 100 mg (+/- 1 mg) of pulverized tissue were prepared and homogenized in 700 µl of iced-cold methanol (80% v/v). In each sample, 25 µl of ribitol at 0.4 $mg.ml^{-1}$ in water were added as internal standard. Samples were incubated 2 h at 4 °C with shaking and then 15 min at 70°C at 850 rpm in a Thermomixer. Tubes were centrifuged 30 min at 12000 rpm and the supernatants were transferred in new tubes. Polar and non-polar phases were separated by the addition of 700 µl of water and 350 µl of chloroform, then vortexed thoroughly and centrifuged for 15 min at 5000 rpm. The upper methanol/water phase (150 µl) was transferred to a new tube and dry in a vacuum centrifuge at RT. Samples were derivatized with 100 µl of methoxamine hydrochloride-HCl (20 $mg.ml^{-1}$ in pyridine) for 90 min at 30°C at 850 rpm in thermomixer and followed by incubation with 100 µL of N,O-bis(trimethylsilyl)trifluoroacetamide (BSTFA) at 80°C during 30 min with shaking at 850 rpm in thermomixer. Finally, samples were injected in split less mode and analyzed using a 7890A gas chromatograph coupled to a 5975C quadrupole mass detector (Agilent Technologies, Palo Alto, CA, USA). In the same manner, 1 µl of retention time standard mixture Supelco C7–C40 saturated alkanes (1,000 $µg.ml^{-1}$ of each component in hexane) diluted 100 fold (10 $µg.ml^{-1}$ final concentration) was injected and analyzed. Alkanes were dissolved in pyridine at 0.22 $mg.ml^{-1}$ final concentration. Chromatic separation was done with a DB-5MS capillary column (30 m × 0.25 mm × 0.25 µm; Agilent J&W Scientific, Folsom, CA, USA). Inlet temperature was set at 280°C. Initial GC Oven temperature was set to 80°C and held for 2 min after injection then GC oven temperature was raised to 300°C at 7°C min^{-1}, and finally held at 300°C for 10 min. Injection and ion source temperatures were adjusted to 300°C and 200°C, respectively with a solvent delay of 5 min. The carrier gas (Helium) flow rate was set to 1 $ml.min^{-1}$. The detector was operated in EI mode at 70 eV and in full scan mode (m/z 33–600).

Metabolites Data Analysis - Compounds were identified by mass spectral and retention time index matching to the mass spectra of the National Institute of Standards and Technology library (NIST20, https://www.nist.gov/) and the Golm Metabolome Database (GMD, http://gmd.mpimp-golm.mpg.de/). Metabolite quantification was performed using MassHunter Software from Agilent. Peaks were deconvoluted and integrated and were normalized to the internal standard ribitol and by the sample weight.

Protein extraction and nanoflow LC-MS analysis

Protein Extraction and Data Acquisition - Kale leaf tissue was harvested at ZT23 and ZT11, flash frozen and ground to a fine powder under liquid N_2 using a mortar and pestle and aliquoted into 400 mg fractions (n = 4; each biological replicate consists of a pool of 3 plants). Samples were then extracted at a 1:2 (w/v) ratio with a solution of 50 mM HEPES-KOH pH 8.0, 50 mM NaCl, and 4% (w/v) SDS. This included vortexing, followed by incubation at 95°C in an Eppendorf microtube table-top shaking incubator shaking at 1100 RPM for 15 mins. This was then followed by an additional 15 mins of shaking at room temperature. All samples

were clarified at 20,000 x g for 5 min at room temperature, with the supernatant retained in fresh Eppendorf microtubes. Sample protein concentrations were measured by bicinchoninic acid (BCA) assay (23225; ThermoScientific), followed by reduction with 10 mM dithiothreitol (DTT) at 95°C for 5 mins. Samples were then cooled and alkylated with 30 mM iodoacetamide (IA) for 30 min in the dark without shaking at room temperature. Subsequently, 10 mM DTT was added to each sample, followed by a quick vortex, and incubation for 10 min at room temperature without shaking. Total proteome peptide pools were generated by sample digestion overnight with 1:100 sequencing grade trypsin (V5113; Promega). Generated peptide pools were quantified by Nanodrop, followed by acidification with formic acid to a final concentration of 5% (v/v) and then dried by vacuum centrifugation. Peptides were then desalted using ZipTip C18 pipette tips (ZTC18S960; Millipore) as previously described [7], dried and dissolved in 3.0% ACN/0.1% FA prior to MS analysis. Digested samples were then analysed using a Fusion Lumos Tribrid Orbitrap mass spectrometer (Thermo Scientific) in a data independent acquisition (DIA) mode using the BoxCarDIA method as previously descried [31]. Dissolved peptides (1 µg) were injected using an Easy-nLC 1200 system (LC140; ThermoScientific) and separated on a 50 cm Easy-Spray PepMap C18 Column (ES903; ThermoScientific). Liquid chromatography and BoxCar DIA acquisition was performed as previously described without deviation (Mehta et al., 2022).

Proteomic Data Analysis – All acquired BoxCar DIA data was analyzed in a library-free DIA approach using Spectronaut v14 (Biognosys AG) using default settings. Data were searched using the *B. oleracea* var *oleracea* proteome (Uniprot: https://www.uniprot.org/containing 58,545 proteins). Default search parameters for proteome quantification were used, with specific search parameters including: a protein, peptide and PSM FDR of 1%, trypsin digestion with 1 missed cleavage, fixed modification including carbamidomethylation of cysteine residues and variable modifications including methionine oxidation. Data was Log2 transformed and globally normalized by median subtraction with significantly changing differentially abundant proteins determined and corrected for multiple comparisons (Bonferroni-corrected *p-value* ≤ 0.05; q-value).

Bioinformatics

Gene Ontology enrichment analyses were performed using the Database for Annotation, Visualization and Integrated Discovery (DAVID; v 6.8; https://david.ncifcrf.gov/home.jsp). Significance was determined using Benjamini-Hochberg (BH) corrected *p-value* ≤ 0.05. Conversion of *B. oleracea var oleracea* gene identifiers to *Arabidopsis* gene identifiers for STRING association network analysis and SUBA4 subcellular localization information retrieval was performed using UniProt (https://www.uniprot.org/). STRING association network analyses were performed in Cytoscape v3.9.0 (https://cytoscape.org/) using the String DB plugin stringApp, all datatypes and a minimum correlation coefficient setting of 0.9. Predicted subcellular localization information was obtained using SUBA4 and the consensus subcellular localization predictor SUBAcon (https://suba.live/). The Eucledian distance *pheatmap* clustered heatmap analysis of diel metabolites was performed in R (3.6.1 R Core Team, 2019). Pathway enrichment was performed using the Plant Metabolic Network (PMN; https://plantcyc.org/) with enrichment determined by a Fisher's exact test significance threshold of *p-value* < 0.01. Additionally figures were assembled using Affinity Designer software (v1.9.1.179; https://affinity.serif.com/en-us/designer/).

Data availability statement

All raw data files, mass spectrometry parameters, and Spectronaut search settings have been uploaded to ProteomeXchange (http://www.proteomexchange.org/) via the PRoteomics IDEntification Database (PRIDE; https://www.ebi.ac.uk/pride/). Project Accession: PXD031780.

Author contributions

Plant growth, phenotyping and harvesting was performed by SS, NB and BC. Metabolite data acquisition and analyses were performed by SS. Proteomics data acquisition and analysis was performed by DM, SS and RGU. The manuscript was written by SS and RGU, with editorial input from DM. All authors contributed to the article and approved the submitted version.

Funding

Funding for this work was generously provided by the Natural Sciences and Engineering Research Council of Canada (NSERC) and Alberta Innovates through their Alliance and Campus Alberta Small Business Engagement (CASBE) funding schemes, respectively. This work was also supported by the Canada Foundation for Innovation (CFI).

Acknowledgments

We would like to thank G2V Optics Inc. for providing their programmable LED lighting system. Thanks to Jack Moore and The Alberta Proteomics and Mass Spectrometry Facility (APM) for providing proteomic support for this work.

Conflict of interest

The authors declare that the research was conducted in the absence of any commercial or financial relationships that could be construed as a potential conflict of interest.

Publisher's note

All claims expressed in this article are solely those of the authors and do not necessarily represent those of their affiliated organizations, or those of the publisher, the editors and the reviewers. Any product that may be evaluated in this article, or claim that may be made by its manufacturer, is not guaranteed or endorsed by the publisher.

Supplementary material

The Supplementary Material for this article can be found online at: https://www.frontiersin.org/articles/10.3389/fpls.2023.1170448/full#supplementary-material

SUPPLEMENTAL DATA SHEET 1
Gas chromatography metabolite data.

SUPPLEMENTAL DATA SHEET 2
Liquid chromatography proteomic data.

SUPPLEMENTAL DATA SHEET 3
Uniprot gene identifier conversion from *Brassica oleracea* to *Arabidopsis*.

SUPPLEMENTAL DATA SHEET 4
PlantCV data and data processing.

SUPPLEMENTAL DATA SHEET 5
MultisynQ phenotype data.

SUPPLEMENTAL DATA SHEET 6
Pathway enrichment analysis using the Plant Metabolic Network (PMN; https://plantcyc.org/.

References

Akram, N. A., Shafiq, F., and Ashraf, M. (2017). Ascorbic acid-a potential oxidant scavenger and its role in plant development and abiotic stress tolerance. *Front. Plant Sci.* 8. doi: 10.3389/fpls.2017.00613

Arias, T., Niederhuth, C. E., McSteen, P., and Pires, J. C. (2021). The molecular basis of kale domestication: transcriptional profiling of developing leaves provides new insights into the evolution of a brassica oleracea vegetative morphotype. *Front. Plant Sci.* 12. doi: 10.3389/fpls.2021.637115

Armenta-Medina, A., Gillmor, C. S., Gao, P., Mora-Macias, J., Kochian, L. V., Xiang, D., et al. (2021). Developmental and genomic architecture of plant embryogenesis: from model plant to crops. *Plant Commun.* 2 (1), 100136. doi: 10.1016/j.xplc.2020.100136

Ayaz, F. A., Glew, R. H., Millson, M., Huang, H. S., Chuang, L. T., Sanz, C., et al. (2006). Nutrient contents of kale (Brassica oleraceae l. var. acephala DC.). *Food Chem.* 96 (4), 572–579. doi: 10.1016/j.foodchem.2005.03.011

Barker, S., Moss, R., and McSweeney, M. B. (2022). Identification of sensory properties driving consumers' liking of commercially available kale and arugula. *J. Sci. Food Agric.* 102 (1), 198–205. doi: 10.1002/jsfa.11346

Becerra-Moreno, A., Alanis-Garza, P. A., Mora-Nieves, J. L., Mora-Mora, J. P., and Jacobo-Velazquez, D. A. (2014). Kale: an excellent source of vitamin c, pro-vitamin a, lutein and glucosinolates. *Cyta-J Food* 12 (3), 298–303. doi: 10.1080/19476337.2013.850743

Bogdanovic, J., Mojovic, M., Milosavic, N., Mitrovic, A., Vucinic, Z., and Spasojevic, I. (2008). Role of fructose in the adaptation of plants to cold-induced oxidative stress. *Eur. Biophys. J.* 37 (7), 1241–1246. doi: 10.1007/s00249-008-0260-9

Carrera, D. A., George, G. M., Fischer-Stettler, M., Galbier, F., Eicke, S., Truernit, E., et al. (2021). Distinct plastid fructose bisphosphate aldolases function in photosynthetic and non-photosynthetic metabolism in arabidopsis. *J. Exp. Bot.* 72 (10), 3739–3755. doi: 10.1093/jxb/erab099

Carvalho, S. D., and Folta, K. M. (2014). Sequential light programs shape kale (Brassica napus) sprout appearance and alter metabolic and nutrient content. *Hortic. Res.* 1, 8. doi: 10.1038/hortres.2014.8

Carvalho, S. D., Schwieterman, M. L., Abrahan, C. E., Colquhoun, T. A., and Folta, K. M. (2016). Light quality dependent changes in morphology, antioxidant capacity, and volatile production in sweet basil (Ocimum basilicum). *Front. Plant Sci.* 7. doi: 10.3389/fpls.2016.01328

Casajus, V., Perini, M., Ramos, R., Lourenco, A. B., Salinas, C., Sanchez, E., et al. (2021). Harvesting at the end of the day extends postharvest life of kale (Brassica oleracea var. sabellica). *Sci. Hortic-Amsterdam* 276 (109757), 1-7. doi: 10.1016/j.scienta.2020.109757

Cervela-Cardona, L., Yoshida, T., Zhang, Y., Okada, M., Fernie, A., and Mas, P. (2021). Circadian control of metabolism by the clock component TOC1. *Front. Plant Sci.* 12. doi: 10.3389/fpls.2021.683516

Chiu, Y. C., Juvik, J. A., and Ku, K. M. (2018). Targeted metabolomic and transcriptomic analyses of "Red russian" kale (Brassicae napus var. pabularia) following methyl jasmonate treatment and larval infestation by the cabbage looper (Trichoplusia ni hubner). *Int. J. Mol. Sci.* 19, (4). doi: 10.3390/ijms19041058

Covington, M. F., Maloof, J. N., Straume, M., Kay, S. A., and Harmer, S. L. (2008). Global transcriptome analysis reveals circadian regulation of key pathways in plant growth and development. *Genome Biol.* 9 (8), R130. doi: 10.1186/gb-2008-9-8-r130

Creux, N., and Harmer, S. (2019). Circadian rhythms in plants. *Cold Spring Harb. Perspect. Biol.* 11, (9). doi: 10.1101/cshperspect.a034611

Dong, N. Q., and Lin, H. X. (2021). Contribution of phenylpropanoid metabolism to plant development and plant-environment interactions. *J. Integr. Plant Biol.* 63 (1), 180–209. doi: 10.1111/jipb.13054

Flis, A., Mengin, V., Ivakov, A. A., Mugford, S. T., Hubberten, H. M., Encke, B., et al. (2019). Multiple circadian clock outputs regulate diel turnover of carbon and nitrogen reserves. *Plant Cell Environ.* 42 (2), 549–573. doi: 10.1111/pce.13440

Francisco, M., and Rodriguez, V. M. (2021). Importance of daily rhythms on brassicaceae phytochemicals. *Agronomy-Basel* 11, (4). doi: 10.3390/agronomy11040639

Galili, G., and Amir, R. (2013). Fortifying plants with the essential amino acids lysine and methionine to improve nutritional quality. *Plant Biotechnol. J.* 11 (2), 211–222. doi: 10.1111/pbi.12025

Gao, P., Quilichini, T. D., Yang, H., Li, Q., Nilsen, K. T., Qin, L., et al. (2022). Evolutionary divergence in embryo and seed coat development of u's triangle brassica species illustrated by a spatiotemporal transcriptome atlas. *New Phytol.* 233 (1), 30–51. doi: 10.1111/nph.17759

Greenham, K., Lou, P., Puzey, J. R., Kumar, G., Arnevik, C., Farid, H., et al. (2017). Geographic variation of plant circadian clock function in natural and agricultural settings. *J. Biol. Rhythms* 32 (1), 26–34. doi: 10.1177/0748730416679307

Han, M., Zhang, C., Suglo, P., Sun, S., Wang, M., and Su, T. (2021). L-aspartate: an essential metabolite for plant growth and stress acclimation. *Molecules* 26, (7). doi: 10.3390/molecules26071887

Hardin, S. C., Winter, H., and Huber, S. C. (2004). Phosphorylation of the amino terminus of maize sucrose synthase in relation to membrane association and enzyme activity. *Plant Physiol.* 134 (4), 1427–1438. doi: 10.1104/pp.103.036780

Haydon, M. J., Mielczarek, O., Robertson, F. C., Hubbard, K. E., and Webb, A. A. (2013). Photosynthetic entrainment of the arabidopsis thaliana circadian clock. *Nature* 502 (7473), 689–692. doi: 10.1038/nature12603

He, M., and Ding, N. Z. (2020). Plant unsaturated fatty acids: multiple roles in stress response. *Front. Plant Sci.* 11. doi: 10.3389/fpls.2020.562785

Hotta, C. T. (2021). From crops to shops: how agriculture can use circadian clocks. *J. Exp. Bot.* 72 (22), 7668–7679. doi: 10.1093/jxb/erab371

Ishihara, H., Moraes, T. A., Pyl, E. T., Schulze, W. X., Obata, T., Scheffel, A., et al. (2017). Growth rate correlates negatively with protein turnover in arabidopsis accessions. *Plant J.* 91 (3), 416–429. doi: 10.1111/tpj.13576

Jeon, J., Kim, J. K., Kim, H., Kim, Y. J., Park, Y. J., Kim, S. J., et al. (2018). Transcriptome analysis and metabolic profiling of green and red kale (Brassica oleracea var. acephala) seedlings. *Food Chem.* 241, 7–13. doi: 10.1016/j.foodchem.2017.08.067

Jin, S. W., Rahim, M. A., Afrin, K. S., Park, J. I., Kang, J. G., and Nou, I. S. (2018). Transcriptome profiling of two contrasting ornamental cabbage (Brassica oleracea var. acephala) lines provides insights into purple and white inner leaf pigmentation. *BMC Genomics* 19 (1), 797. doi: 10.1186/s12864-018-5199-3

Joshi, V., Joung, J. G., Fei, Z., and Jander, G. (2010). Interdependence of threonine, methionine and isoleucine metabolism in plants: accumulation and transcriptional regulation under abiotic stress. *Amino Acids* 39 (4), 933–947. doi: 10.1007/s00726-010-0505-7

Kim, J. A., Kim, H. S., Choi, S. H., Jang, J. Y., Jeong, M. J., and Lee, S. I. (2017). The importance of the circadian clock in regulating plant metabolism. *Int. J. Mol. Sci.* 18, (12). doi: 10.3390/ijms18122680

Klopsch, R., Baldermann, S., Voss, A., Rohn, S., Schreiner, M., and Neugart, S. (2019). Narrow-banded UVB affects the stability of secondary plant metabolites in kale (Brassica oleracea var. sabellica) and pea (Pisum sativum) leaves being added to lentil flour fortified bread: a novel approach for producing functional foods. *Foods* 8, (10). doi: 10.3390/foods8100427

Krahmer, J., Hindle, M., Perby, L. K., Mogensen, H. K., Nielsen, T. H., Halliday, K. J., et al. (2022). The circadian clock gene circuit controls protein and phosphoprotein rhythms in arabidopsis thaliana. *Mol. Cell Proteomics* 21 (1), 100172. doi: 10.1016/j.mcpro.2021.100172

Kromdijk, J., Glowacka, K., Leonelli, L., Gabilly, S. T., Iwai, M., Niyogi, K. K., et al. (2016). Improving photosynthesis and crop productivity by accelerating recovery from photoprotection. *Science* 354 (6314), 857–861. doi: 10.1126/science.aai8878

Kuhlgert, S., Austic, G., Zegarac, R., Osei-Bonsu, I., Hoh, D., Chilvers, M. I., et al. (2016). MultispeQ beta: a tool for large-scale plant phenotyping connected to the open PhotosynQ network. *R Soc. Open Sci.* 3 (10), 160592. doi: 10.1098/rsos.160592

Liu, Y., Feng, X., Zhang, Y., Zhou, F., and Zhu, P. (2021). Simultaneous changes in anthocyanin, chlorophyll, and carotenoid contents produce green variegation in pink-leaved ornamental kale. *BMC Genomics* 22 (1), 455. doi: 10.1186/s12864-021-07785-x

Liu, X. S., Yang, X., Wang, L. M., Duan, Q. Q., and Huang, D. F. (2016). Comparative analysis of metabolites profile in spinach (Spinacia oleracea l.) affected by different concentrations of gly and nitrate. *Sci. Hortic-Amsterdam* 204, 8–15. doi: 10.1016/j.scienta.2016.02.037

Liu, X., Zhang, B., Wu, J., Li, Z., Han, F., Fang, Z., et al. (2020). Pigment variation and transcriptional response of the pigment synthesis pathway in the S2309 triple-color ornamental kale (Brassica oleracea l. var. acephala) line. *Genomics* 112 (3), 2658–2665. doi: 10.1016/j.ygeno.2020.02.019

Maiwald, D., Dietzmann, A., Jahns, P., Pesaresi, P., Joliot, P., Joliot, A., et al. (2003). Knock-out of the genes coding for the rieske protein and the ATP-synthase delta-subunit of arabidopsis. effects on photosynthesis, thylakoid protein composition, and nuclear chloroplast gene expression. *Plant Physiol.* 133 (1), 191–202. doi: 10.1104/pp.103.024190

Megias-Perez, R., Hahn, C., Ruiz-Matute, A. I., Behrends, B., Albach, D. C., and Kuhnert, N. (2020). Changes in low molecular weight carbohydrates in kale during development and acclimation to cold temperatures determined by chromatographic techniques coupled to mass spectrometry. *Food Res. Int.* 127, 108727. doi: 10.1016/j.foodres.2019.108727

Mehta, D., Krahmer, J., and Uhrig, R. G. (2021). Closing the protein gap in plant chronobiology. *Plant J.* 106 (6), 1509–1522. doi: 10.1111/tpj.15254

Mehta, D., Scandola, S., and Uhrig, R. G. (2022). BoxCar and library-free data-independent acquisition substantially improve the depth, range, and completeness of label-free quantitative proteomics. *Anal. Chem.* 94 (2), 793–802. doi: 10.1021/acs.analchem.1c03338

Migliozzi, M., Thavarajah, D., Thavarajah, P., and Smith, P. (2015). Lentil and kale: complementary nutrient-rich whole food sources to combat micronutrient and calorie malnutrition. *Nutrients* 7 (11), 9285–9298. doi: 10.3390/nu7115471

Moing, A., Allwood, J. W., Aharoni, A., Baker, J., Beale, M. H., Ben-Dor, S., et al. (2020). Comparative metabolomics and molecular phylogenetics of melon (Cucumis melo, cucurbitaceae) biodiversity. *Metabolites* 10, (3). doi: 10.3390/metabo10030121

Muller, N. A., Wijnen, C. L., Srinivasan, A., Ryngajllo, M., Ofner, I., Lin, T., et al. (2016). Domestication selected for deceleration of the circadian clock in cultivated tomato. *Nat. Genet.* 48 (1), 89–93. doi: 10.1038/ng.3447

Munnik, T., Irvine, R. F., and Musgrave, A. (1998). Phospholipid signalling in plants. *Biochim. Biophys. Acta* 1389 (3), 222–272. doi: 10.1016/s0005-2760(97)00158-6

Nemzer, B., Al-Taher, F., and Abshiru, N. (2021). Extraction and natural bioactive molecules characterization in spinach, kale and purslane: a comparative study. *Molecules* 26 (9), 2515. doi: 10.3390/molecules26092515

Neugart, S., and Bumke-Vogt, C. (2021). Flavonoid glycosides in brassica species respond to UV-b depending on exposure time and adaptation time. *Molecules* 26 (9), 494. doi: 10.3390/molecules26020494

Neugart, S., Fiol, M., Schreiner, M., Rohn, S., Zrenner, R., Kroh, L. W., et al. (2014). Interaction of moderate UV-b exposure and temperature on the formation of structurally different flavonol glycosides and hydroxycinnamic acid derivatives in kale (Brassica oleracea var. sabellica). *J. Agric. Food Chem.* 62 (18), 4054–4062. doi: 10.1021/jf4054066

Neugart, S., Krumbein, A., and Zrenner, R. (2016). Influence of light and temperature on gene expression leading to accumulation of specific flavonol glycosides and hydroxycinnamic acid derivatives in kale (Brassica oleracea var. *sabellica). Front. Plant Sci.* 7. doi: 10.3389/fpls.2016.00326

Paciolla, C., Fortunato, S., Dipierro, N., Paradiso, A., De Leonardis, S., Mastropasqua, L., et al. (2019). Vitamin c in plants: from functions to biofortification. *Antioxidants-Basel* 8 (11), 519. doi: 10.3390/antiox8110519

Pongrac, P., Fischer, S., Thompson, J. A., Wright, G., and White, P. J. (2019). Early responses of brassica oleracea roots to zinc supply under sufficient and Sub-optimal phosphorus supply. *Front. Plant Sci.* 10. doi: 10.3389/fpls.2019.01645

R Core Team. (2019). *R: A Language and Environment for Statistical Computing*. R Foundation for Statistical Computing, Vienna, Austria. Available at: https://www.R-project.org/.

Reda, T., Thavarajah, P., Polomski, R., Bridges, W., Shipe, E., and Thavarajah, D. (2021). Reaching the highest shelf: a review of organic production, nutritional quality, and shelf life of kale (Brassica oleracea var. acephala). *Plants People Planet* 3 (4), 308–318. doi: 10.1002/ppp3.10183

Rees, H., Joynson, R., Brown, J. K. M., and Hall, A. (2021). Naturally occurring circadian rhythm variation associated with clock gene loci in Swedish arabidopsis accessions. *Plant Cell Environ.* 44 (3), 807–820. doi: 10.1111/pce.13941

Rennie, E. A., and Scheller, H. V. (2014). Xylan biosynthesis. *Curr. Opin. Biotechnol.* 26, 100–107. doi: 10.1016/j.copbio.2013.11.013

Romanowski, A., Schlaen, R. G., Perez-Santangelo, S., Mancini, E., and Yanovsky, M. J. (2020). Global transcriptome analysis reveals circadian control of splicing events in arabidopsis thaliana. *Plant J.* 103 (2), 889–902. doi: 10.1111/tpj.14776

Ruts, T., Matsubara, S., Wiese-Klinkenberg, A., and Walter, A. (2012). Diel patterns of leaf and root growth: endogenous rhythmicity or environmental response? *J. Exp. Bot.* 63 (9), 3339–3351. doi: 10.1093/jxb/err334

Samec, D., Urlic, B., and Salopek-Sondi, B. (2019). Kale (Brassica oleracea var. acephala) as a superfood: review of the scientific evidence behind the statement. *Crit. Rev. Food Sci.* 59 (15), 2411–2422. doi: 10.1080/10408398.2018.1454400

Sanchez, S. E., Rugnone, M. L., and Kay, S. A. (2020). Light perception: a matter of time. *Mol. Plant* 13 (3), 363–385. doi: 10.1016/j.molp.2020.02.006

Scandola, S., Mehta, D., Li, Q., Rodriguez Gallo, M. C., Castillo, B., and Uhrig, R. G. (2022). Multi-omic analysis shows REVEILLE clock genes are involved in carbohydrate metabolism and proteasome function. *Plant Physiol.* 190 (2), 1005-1023. doi: 10.1093/plphys/kiac269

Schulze, S., Westhoff, P., and Gowik, U. (2016). Glycine decarboxylase in C3, C4 and C3-C4 intermediate species. *Curr. Opin. Plant Biol.* 31, 29–35. doi: 10.1016/j.pbi.2016.03.011

Shahidi, F., and Ambigaipalan, P. (2018). Omega-3 polyunsaturated fatty acids and their health benefits. *Annu. Rev. Food Sci. T* 9, 345–381. doi: 10.1146/annurev-food-111317-095850

Shi, L. Y., Cao, S. F., Shao, J. R., Chen, W., Zheng, Y. H., Jiang, Y. M., et al. (2014). Relationship between sucrose metabolism and anthocyanin biosynthesis during ripening in Chinese bayberry fruit. *J. Agr Food Chem.* 62 (43), 10522–10528. doi: 10.1021/jf503317k

Somers, D. E., Devlin, P. F., and Kay, S. A. (1998). Phytochromes and cryptochromes in the entrainment of the arabidopsis circadian clock. *Science* 282 (5393), 1488–1490. doi: 10.1126/science.282.5393.1488

Steed, G., Ramirez, D. C., Hannah, M. A., and Webb, A. A. R. (2021). Chronoculture, harnessing the circadian clock to improve crop yield and sustainability. *Science* 372 (6541), eabc9141. doi: 10.1126/science.abc9141

Stein, O., and Granot, D. (2019). An overview of sucrose synthases in plants. *Front. Plant Sci.* 10. doi: 10.3389/fpls.2019.00095

Steppe, K., Sterck, F., and Deslauriers, A. (2015). Diel growth dynamics in tree stems: linking anatomy and ecophysiology. *Trends Plant Sci.* 20 (6), 335–343. doi: 10.1016/j.tplants.2015.03.015

Thavarajah, D., Thavarajah, P., Abare, A., Basnagala, S., Lacher, C., Smith, P., et al. (2016). Mineral micronutrient and prebiotic carbohydrate profiles of USA -grown kale (Brassica oleracea l. var. acephala). *J. Food Compos Anal.* 52, 9–15. doi: 10.1016/j.jfca.2016.07.003

Tohge, T., Watanabe, M., Hoefgen, R., and Fernie, A. R. (2013). Shikimate and phenylalanine biosynthesis in the green lineage. *Front. Plant Sci.* 4. doi: 10.3389/fpls.2013.00062

Uhrig, R. G., Echevarria-Zomeno, S., Schlapfer, P., Grossmann, J., Roschitzki, B., Koerber, N., et al. (2021). Diurnal dynamics of the arabidopsis rosette proteome and phosphoproteome. *Plant Cell Environ.* 44 (3), 821–841. doi: 10.1111/pce.13969

Uhrig, R. G., Schlapfer, P., Roschitzki, B., Hirsch-Hoffmann, M., and Gruissem, W. (2019). Diurnal changes in concerted plant protein phosphorylation and acetylation in arabidopsis organs and seedlings. *Plant J.* 99 (1), 176–194. doi: 10.1111/tpj.14315

Wang, Q., Zuo, Z., Wang, X., Liu, Q., Gu, L., Oka, Y., et al. (2018). Beyond the photocycle-how cryptochromes regulate photoresponses in plants? *Curr. Opin. Plant Biol.* 45 (Pt A), 120–126. doi: 10.1016/j.pbi.2018.05.014

Waterland, N. L., Moon, Y., Tou, J. C., Kopsell, D. A., Kim, M. J., and Park, S. (2019). Differences in leaf color and stage of development at harvest influenced phytochemical content in three cultivars of kale (Brassica oleracea l. and b. napus). *J. Agric. Sci.* 11 (3). doi: 10.5539/jas.v11n3p14

Xiao, Y., Chu, L., Zhang , Y., Bian, Y., Xiao, J., Xu, D., et al. (2002). HY5: A Pivotal Regulator of Light-Dependent Development in Higher Plants. *Front Plant Sci.* 12, 800989. doi: 10.3389/fpls.2021.800989

Xing, S., and Poirier, Y. (2012). The protein acetylome and the regulation of metabolism. *Trends Plant Sci.* 17 (7), 423–430. doi: 10.1016/j.tplants.2012.03.008

Xu, X., Yuan, L., Yang, X., Zhang, X., Wang, L., and Xie, Q. (2022). Circadian clock in plants: linking timing to fitness. *J. Integr. Plant Biol.* 64 (4), 792–811. doi: 10.1111/jipb.13230

Zhao, W., Liu, H., Zhang, L., Hu, Z., Liu, J., Hua, W., et al. (2019). Genome-wide identification and characterization of FBA gene family in polyploid crop brassica napus. *Int. J. Mol. Sci.* 20 (22), 5749. doi: 10.3390/ijms20225749

Zhu, J. H., Fu, X. M., Koo, Y. D., Zhu, J. K., Jenney, F. E., Adams, M. W. W., et al. (2007). An enhancer mutant of arabidopsis salt overly sensitive 3 mediates both ion homeostasis and the oxidative stress response. *Mol. Cell Biol.* 27 (14), 5214–5224. doi: 10.1128/Mcb.01989-06